Entanglement production in colliding wave packets

C. K. Law
Department of Physics, The Chinese University of Hong Kong, Shatin, Hong Kong SAR, China
(Received 30 August 2004; published 10 December 2004)

We study the generation of quantum entanglement in two-particle scattering processes. When two wave packets collide, we discover that entanglement grows appreciably because of the interference between the incident and scattered waves. After the collision, quantum entanglement is mainly governed by the scattering phase shift and the widths of the incident wave packets. For interaction potentials that exhibit scattering resonance, we show that quantum entanglement can be enhanced near resonance energies.

DOI: 10.1103/PhysRevA.70.062311 PACS number(s): 03.67.Mn, 03.65.Ud

Generation of quantum entanglement between two spatially separated particles requires nonlocal interactions that build up quantum correlations dynamically [1,2]. In recent years, the dynamics of two-particle entanglement has been discussed in various physical situations. For example, continuous-variable entanglement in photon-atom scattering [3], photoionization processes [4–7], trapped atom pairs [8], and classically chaotic systems [9,10], have been studied. Conceptually, the simplest mechanism of entangling two particles is by scattering. Because of mutual interactions, the two particles can become entangled as they approach each together. After the collision, the two particles may still be entangled and share some forms of quantum information in the final (scattered) states. However, much remains unclear about the nature of such entanglement and how the interaction potentials and particle energies control the entanglement. In addition, the interesting role of scattering resonance in entanglement production has not been explored.

To address these issues, we investigate a system of two colliding particles (A and B) in a one-dimensional free space. One-dimensional models allow us to study the quantum dynamics in detail, and they demonstrate some interesting and general features that may shed light on more complicated three-dimensional problems. In this paper we examine the time development of entanglement with various short range interaction potentials. We will show that there exists a transient period during which quantum entanglement changes significantly. After the completion of scattering, the final entanglement is determined by the nonlinearity of wave vector dependence on the scattering phase angle. In addition, for interaction potentials that allow scattering resonances, we show that entanglement can be enhanced at the corresponding resonance energies.

To begin with, we indicate that quantum entanglement of a general two-particle system (in a pure state) can be characterized by the purity function $\mathcal{P}(t)=\mathrm{Tr}[\rho_A(t)^2]$, where $\rho_A(t)=\mathrm{Tr}_B[\rho(t)]$ is the reduced density of the particle A, and $\rho(t)$ is the whole $(A+B)$ density matrix at time t. To quantify the entanglement, it is more convenient to employ the inverse of $\mathcal{P}(t)$, i.e.,

$$\mathcal{K}(t) = 1/\mathcal{P}(t), \tag{1}$$

which measures the effective number of Schmidt modes [4]. The larger the value of $\mathcal{K}$, the higher the entanglement. A disentangled (product) state corresponds to $\mathcal{K}=1$. Bell states of two-photon polarization have $\mathcal{K}=2$. For continuous systems, $\mathcal{K}$ can in principle be very large because of the vast Hilbert space involved. The main constraint comes from the conservation of energy and momentum which restricts accessible phase space. In atomic physics, $\mathcal{K}$ has also been employed to indicate the important role of two-body correlations in various dynamical processes [5,11].

In this paper, we will focus on a system of particles with equal mass. Using the center of mass and relative coordinates $X=(x_A+x_B)/2$ and $x=x_A-x_B$, the Hamiltonian of the system is given by

$$H = \frac{P^2}{2M} + \frac{p^2}{2\mu} + V(|x|), \tag{2}$$

where $P=p_A+p_B$ and $p=(p_A-p_B)/2$ are the momentum of the center of mass and relative coordinates, respectively. The interaction potential $V(|x_A-x_B|)$ is a function of the distance between the particles. For convenience, we will adopt the units $\hbar=m=1$, so that the center mass is $M=2$ and the reduced mass is $\mu=1/2$. Since the center of mass and relative coordinates are uncoupled in the Hamiltonian, the two-particle wave function at time t takes the form $\Psi(x_A,x_B,t)=\Psi_c(X,t)\Psi_r(x,t)$, if the initial state can be factorized into a product of a center mass part and a relative coordinate part.

Let us first discuss a simple hard-wall model, which is a one-dimensional analog of the hard-sphere potential problem. In this case, the interaction potential $V(x)=0$ for $|x|>a$ and $V(x)=\infty$ for $|x|<a$, where $a/2$ is the size of each particle. Initially, particle A (B) is described by a localized wave packet at the position q_0 ($-q_0$) with an averaged momentum $-\hbar k_0$ ($+\hbar k_0$). We assume that q_0 is large compared with a and the initial width of the wave packets. Because the particles are impenetrable, the two-particle wave function is mainly confined in the $x>a$ domain at any time. It is not difficult to construct a solution that satisfies the Schrödinger equation with the boundary condition $\Psi_r(a,t)=0$:

$$\Psi(x_A,x_B,t) = [f_-(x_A,t)f_+(x_B,t) - f_+(x_A-a,t)f_-(x_B+a,t)]\,\theta(x_A-x_B-a). \tag{3}$$

Here $\theta(\xi)$ is a step function, and f_+ and f_- are free Gaussian wave packets propagating in the right and left directions:

 ©2004 The American Physical Society

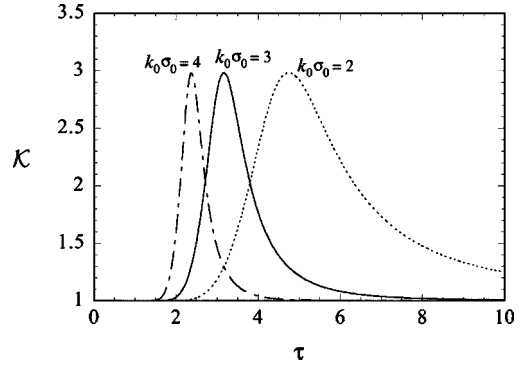

FIG. 1. $\mathcal{K}$ as a function of dimensionless time τ for various incident velocities in the hard-wall problem. The initial wave packet separation is $2q_0=20\sigma_0$. The dimensionless quantity $k_0\sigma_0$ is proportional to the incident speed. All the three curves correspond to the same initial wave packet width σ_0.

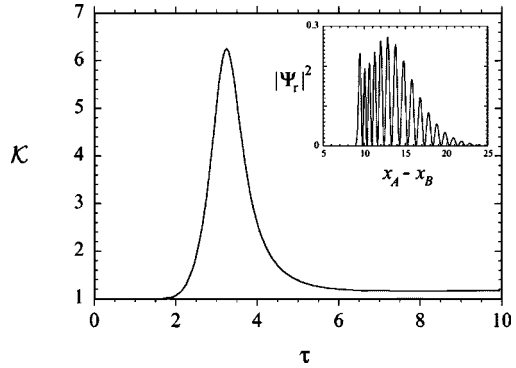

FIG. 2. An illustration of the time dependence of $\mathcal{K}$ in the Morse potential problem with the initial wave packet parameters $k_0\sigma_0=3$ and $q_0=30\sigma_0$. The parameters of the potential are $a=\sigma_0$, $x_0=10\sigma_0$, $V_0=24\hbar^2/m\sigma_0^2$. The inset shows the absolute square of the relative coordinate wave function when $\mathcal{K}$ reaches the maximum.

$$f_{\pm}(\xi,t)=\left(\frac{2}{\pi}\right)^{1/4}\sqrt{\frac{\sigma_0}{\sigma^2(t)}}\exp\left[-\frac{(\xi\pm q_0\mp k_0t)^2}{\sigma^2(t)}\pm ik_0\xi - i\frac{k_0^2}{2}t\right], \tag{4}$$

where $\sigma^2(t)=\sigma_0^2+2it$ with σ_0 being the initial spread of the wave packets. Since $q_0\gg a,\sigma_0$, the initial state $\Psi(x_A,x_B,0)\approx f_-(x_A,0)f_+(x_B,0)$ is a disentangled state. The long time behavior of $\Psi(x_A,x_B,t)$ is described by the $f_+(x_A-a,t)f_-(x_B+a,t)$ term which corresponds to the reflected waves due to scattering.

With the help of the solution (3), we can calculate the purity function and hence the time development of the entanglement. The expression of $\mathcal{P}(t)$ is calculated from the integral

$$\mathcal{P}(t)=\int\int\int\int \Psi^*(x_A,x_B',t)\Psi^*(x_A',x_B,t) \times\Psi(x_A,x_B,t)\Psi(x_A',x_B',t)dx_Adx_A'dx_Bdx_B'. \tag{5}$$

Such an integral does not have a simple analytic form. We carry out numerical calculations, and the typical behavior of $\mathcal{K}$ is shown in Fig. 1. For convenience, we plot with the dimensionless time $\tau=\hbar t/2\mu\sigma_0^2$. We notice that the increase and decrease of entanglement occur in a transient period. Such a period corresponds to the time interval during which the incident and the reflected wave packets interfere most. It can be seen from Eq. (3) that the incident part $f_-(x_A,t)f_+(x_B,t)$ and the reflected part $f_+(x_A-a,t)f_-(x_B+a,t)$ are product states. It is only when both parts are superimposed that entanglement is generated.

In Fig. 1, $\mathcal{K}$ reaches a peak value at $\tau_0=(2q_0-a)/2k_0\sigma_0^2$ [or equivalently the time $t_0=(2q_0-a)m/2\hbar k_0$]. This is the instant when the centers of the incident wave packets are separated by a. We notice that the peak value is insensitive to the incident wave vector k_0. In fact, if k_0 is sufficiently large such that $k_0\sigma_0\gg1$ or $k_0q_0\gg1$, we find that the peak value of $\mathcal{K}$ is given by

$$\mathcal{K}(\tau_0)\approx 3. \tag{6}$$

This result can be derived analytically for Gaussian wave functions. According to Eq. (4), $\Psi(x_A,x_B,t_0)=\mathcal{N}\psi(x_A)\psi^*(x_B)\sin[k_0(a-x_A+x_B)]\theta(x_A-x_B-a)$, where ψ is a Gaussian function and $\mathcal{N}$ is a normalization constant. Quantum correlation between the particles is described by the interference term $\sin[k_0(a-x_A+x_B)]$, which depends only on the relative coordinate. In the case where k_0 is large as stated, we can carry out the integral (5) approximately by discarding fast oscillatory (spatial) terms [12]. The four step functions that would appear in the integral (5) can be taken care of by using the symmetry property of the wave function (3). The result is an interesting integer value 3, which agrees very well with the numerical calculations in Fig. 1.

Transient entanglement arising from quantum interference between the incident and the scattered wave packets is also observed in various interaction potentials with a dominant repulsive core. For example, we have examined a more realistic potential for atom-atom interactions, namely, the Morse potential $V(x)=V_0(e^{-2a(x-x_0)}-2e^{-a(x-x_0)})$, where x_0 is the minimum potential position, and V_0 and a are the strength and range of the potential, respectively. The Morse potential is attractive for $x>x_0$, but becomes strongly repulsive for $x\ll x_0$. With initial Gaussian wave packets $f_-(x_A,0)$ and $f_+(x_B,0)$, we employ the split-operator method to obtain the time-dependent wave function.

In Fig. 2, a typical $\mathcal{K}$ is illustrated as a function of time. Similar to the hard-wall problem, $\mathcal{K}$ reaches a maximum when strong interference between the incident and reflected waves occurs (see the inset). However, the peak value of $\mathcal{K}$ can be substantially higher than 3. The reasons are complicated by the existence of bound states and interference effects involving nontrivial wave packet spreading inside the potential well. In addition, the main phase factors of Ψ_r are no longer $e^{\pm ik_0x}$, but are approximated by $\exp(\pm i\int^x\sqrt{E-V(\xi)}d\xi)$ (where E is the energy), according to the WKB argument. The nonlinear position dependence in the phase would cause extra cancellations in the integral (5) and hence reduce the purity value [12].

An important feature shown in Fig. 2 is that $\mathcal{K}$ is greater than 1 in the final state, i.e., the two particles are entangled after the scattering is completed. This is in sharp contrast to the hard-wall problem in which the final state $f_+(x_A-a,t)f_-(x_B+a,t)$ is disentangled. This phenomenon can be analyzed by studying the scattering phase factor in the long time limit. Let us consider a general short range potential with an impenetrable hard core. For elastic scattering, the long time two-particle wave function in momentum space takes the general form

$$\Phi(k_A,k_B,t)=\tilde{f}_-(-k_A)e^{-ik_A^2t/2}\tilde{f}_+(-k_B)e^{-ik_B^2t/2}e^{i\phi(k_A,k_B)}, \quad (7)$$

where $\tilde{f}_\pm$ is the spatial Fourier transform of the initial wave packets $f_\pm$, and $\phi(k_A,k_B)$ is the scattering phase angle. The negative signs in the argument of $\tilde{f}_\pm$ are due to the change of propagation directions after the scattering, assuming $k_A>0$ and $k_B<0$.

The purity of the state (7) is given by

$$\mathcal{P}=\int\int\int\int dk_A dk_A' dk_B dk_B' |\tilde{f}_-(-k_A)|^2|\tilde{f}_+(-k_B)|^2 \times|\tilde{f}_-(-k_A')|^2|\tilde{f}_+(-k_B')|^2\times\exp\{i[\phi(k_A,k_B)+\phi(k_A',k_B')-\phi(k_A,k_B')-\phi(k_A',k_B)]\}. \quad (8)$$

Therefore the purity function and the scattering phase angle are related. We note that $\phi(k_A,k_B)=\phi[(k_A-k_B)/2]$ is a function of k_A-k_B, because of the separability of the Hamiltonian (2). In the case of the hard-wall problem, $\phi(k)$ is purely a linear function of k and hence the exponent in Eq. (8) is zero. This explains why $\mathcal{P}=1$ (i.e., disentangled states) for the hard-wall problem. For general potentials, $\phi(k)$ depends on k nonlinearly, and hence the phase angles in the exponent cannot be completely cancelled. In other words, the nonlinear property of the scattering phase shift is the key to the generation of entanglement in scattering processes [13].

If the variation of ϕ is small within the width of $\tilde{f}_\pm(k)$ [or equivalently the width of $\tilde{f}_\pm(k)$ is sufficiently narrow], we may expand ϕ around the peak at $k_A=k_0$, $k_B=-k_0$, i.e.,

$$\phi(\xi)\approx\phi(\bar{\xi})+\phi'(\bar{\xi})(\xi-\bar{\xi})+\phi''(\bar{\xi})(\xi-\bar{\xi})^2/2, \quad (9)$$

where $\xi=(k_A-k_B)/2$ and $\bar{\xi}=k_0$. In this way the combinations of phase angles in Eq. (8) can be reduced to a simple expression that is proportional to the second derivative $\phi''(\bar{\xi})$,

$$\phi\left(\frac{k_A-k_B}{2}\right)+\phi\left(\frac{k_A'-k_B'}{2}\right)-\phi\left(\frac{k_A-k_B'}{2}\right)-\phi\left(\frac{k_A'-k_B}{2}\right)\approx-\frac{\phi''(k_0)}{4}(k_A-k_A')(k_B-k_B'). \quad (10)$$

For Gaussian $\tilde{f}_\pm$, a direct integration gives an approximate expression of $\mathcal{K}$,

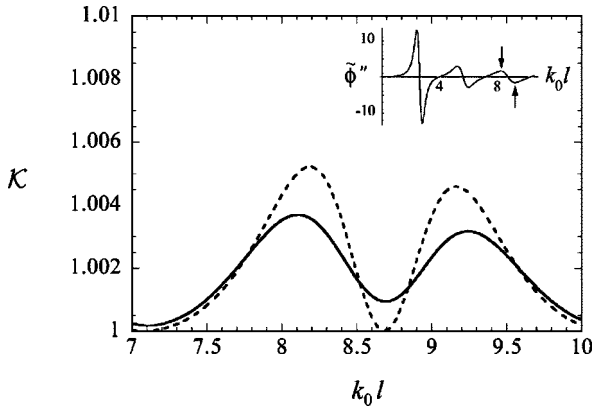

FIG. 3. Long time value of $\mathcal{K}$ as a function of incident wave number in the cavity potential problem. The solid line is obtained by numerical integration of (8); the dashed line corresponds to the approximation formula (11). The potential parameter is $g=3\hbar^2/ml$, where $l=l_0-a$. The wave packet has an initial width $\sigma_0=2\sqrt{2}l$. The inset shows the dimensionless second derivative $\tilde{\phi}''\equiv l^{-2}d^2\phi/dk^2$ of the scattering phase angle.

$$\mathcal{K}\approx\sqrt{1+[\phi''(k_0)/2\sigma_0^2]^2}. \quad (11)$$

This expression indicates how the degree of entanglement is controlled by $\phi''(k_0)$ and the widths of the incident wave packets.

The nonlinear dependence of k in $\phi(k)$ is responsible for the generation of entanglement. For potentials that allow quasibound states or resonances, $\phi(k)$ can be a highly nonlinear function of k. This suggests an interesting mechanism that quantum entanglement can be enhanced near scattering resonances. We illustrate this phenomenon in a "cavity" potential model: $V(x)=g\delta(x-l_0)$ for $|x|>a$ and $V(x)=\infty$ for $|x|<a$, where $g>0$ is the strength of the δ-function potential at $x=l_0>a$. In this model, the hard wall at $x=a$ and the δ-function potential form a cavity for matter waves. The scattering phase factor can be calculated analytically, and reads

$$e^{i\phi(k)}=e^{-2ikl_0}\frac{-ik\cos[k(l_0-a)]+(k-ig)\sin[k(l_0-a)]}{ik\cos[k(l_0-a)]+(k+ig)\sin[k(l_0-a)]}. \quad (12)$$

When g is sufficiently large, quasibound states appear at $k\approx n\pi/(l_0-a)$ with n being positive integers.

In Fig. 3 we illustrate the long time $\mathcal{K}$ value as a function of the incident wave number k_0. The range of k_0 shown corresponds to the third resonance zone where ϕ'' has two maxima (indicated by arrows in the inset). Therefore $\mathcal{K}$ is expected to display two peaks according to the estimation (11). Our numerical calculations (solid line), which were performed without employing the approximation (9), confirm the doublet feature. In fact we also observe doublets at the first and second resonances (not shown). However, we remark that Eq. (11) serves only as a guide to locate the resonance. Its validity depends on the quadratic phase approxi-

mation (9), which requires narrow bandwidths in the momentum space. Therefore the discrepancy between exact results and Eq. (11) could be expected.

In summary, we have examined several features of entanglement generated in wave packet scattering processes. For interaction potentials with a strong repulsive core, quantum interference between the incident and reflected waves can generate a transient entanglement. The peak value of $\mathcal{K}$ is close to an integer 3 for the hard-wall model, and higher peak values of $\mathcal{K}$ are observed numerically in a Morse potential. Quite generally, the two particles can become entangled after the collision. We establish a relation between the long time $\mathcal{K}$ value and the scattering phase shift $\phi(k)$. If $\phi(k)$ is a linear function of k, there is no entanglement in the final state. We note that this feature is not limited to the hard-wall problem, because $\phi(k)$ is typically linear at high energies $\hbar^2 k/\mu a \gg V$ for potentials with a short range a. Therefore entanglement production is more significant in low-energy regimes, for example, in collisions of cold atoms. Our analysis also indicates that the strong nonlinearity in $\phi(k)$ around the scattering resonance can be exploited to enhance entanglement. However, in order to resolve the resonance, incident wave packets should have a narrow energy spread, i.e., a large initial spread σ_0. This would limit the value of $\mathcal{K}$ according to the estimation (11). Hence the idea of resonance enhancement should be understood in a relative sense, referring to the increase of $\mathcal{K}$ when σ_0 is fixed.

This work is a step toward addressing interesting dynamics of entanglement in scattering processes, and further investigations with more realistic models would be needed. Comparing with three-dimensional situations, our one-dimensional study has the limitation that angular correlations are omitted. However, we remark that if one could choose to observe scattered waves in two opposite directions only, then the relevant quantum state may be analyzed by a one-dimensional treatment. In this case, our result implies that the scattering phase shift is a crucial quantity to determine quantum entanglement.

The author thanks Professor J. H. Eberly and Professor M.-C. Chu for discussions. This work is supported in part by the Research Grants Council of the Hong Kong Special Administrative Region, China (Project Nos. 400504 and 423701).

[1] O. Kübler and H. D. Zeh, Ann. Phys. (N.Y.) **76**, 405 (1973).
[2] W. Dur, G. Vidal, J. I. Cirac, N. Linden, and S. Popescu, Phys. Rev. Lett. **87**, 137901 (2001).
[3] K. W. Chan, C. K. Law, and J. H. Eberly, Phys. Rev. A **68**, 022110 (2003).
[4] R. Grobe, K. Rzążewski, and J. H. Eberly, J. Phys. B **27**, L503 (1994).
[5] W.-C. Liu, J. H. Eberly, S. L. Haan, and R. Grobe, Phys. Rev. Lett. **83**, 520 (1999).
[6] N. Chandra and R. Ghosh, Phys. Rev. A **69**, 012315 (2004).
[7] M. V. Fedorov, M. A. Efremov, A. E. Kazakov, K. W. Chan, C. K. Law, and J. H. Eberly, Phys. Rev. A **69**, 052117 (2004).
[8] H. Mack and M. Freyberger, Phys. Rev. A **66**, 042113 (2002).
[9] P. A. Miller and S. Sarkar, Phys. Rev. E **60**, 1542 (1999); A. Tanaka, H. Fujisaki, and T. Miyadera, *ibid.* **66**, 045201 (2002); H. Fujisaki, T. Miyadera, and A. Tanaka, *ibid.* **67**, 066201 (2003); X.-W. Hou and B. Hu, Phys. Rev. A **69**, 042110 (2004).
[10] Ph. Jacquod, Phys. Rev. Lett. **92**, 150403 (2004).
[11] R. E. Wagner, P. J. Peverly, Q. Su, and R. Grobe, Laser Phys. **11**, 221 (2001).
[12] In the hard-wall problem, the integral (5) at time t_0 involves an interference term: $\sin k_0(x_1-x_2)\sin k_0(x_3-x_4)\sin k_0(x_1-x_4)\sin k_0(x_2-x_3)=1/8+$(spatial oscillation terms), where $x_1=x_A-a/2$, $x_2=x_B+a/2$, $x_3=x'_A-a/2$, and $x_4=x'_B+a/2$. The oscillatory terms have negligible contribution to the integral in the large k_0 limit. Note that the constant $1/8$ comes from the linearity of $k_0 x$ in the sine function.
[13] Observable effects of entanglement due to phases in Gaussian states were discussed recently by K. W. Chan and J. H. Eberly, e-print quant-ph/0404093.